A simple method for preparation of molecularly imprinted nanofiber materials with signal transduction ability†

Keiichi Yoshimatsu,[a] Lei Ye,*[a] Patrik Stenlund[b] and Ioannis S. Chronakis*[b]

Received (in Cambridge, UK) 20th December 2007, Accepted 31st January 2008
First published as an Advance Article on the web 20th February 2008
DOI: 10.1039/b719586a

A simple electrospinning method is developed to introduce signal transduction ability into molecularly imprinted nanofibers.

Molecularly imprinted polymers (MIPs) are synthetic polymer materials having tailor-made molecular recognition abilities.[1] Compared to biological receptors (*e.g.* antibodies, enzymes, *etc.*) that are commonly used in bioanalysis, MIPs have far higher chemical and physical stabilities[2] and can be easily synthesized on a large scale. Due to these desirable properties, MIPs are attracting increasing attention to be used as recognition elements for development of new analytical assays and chemical sensors,[3] and also new logic gates selective for predetermined chemical inputs.[4] In addition to improving binding affinity and specificity of MIPs, an important research topic is to introduce signal transduction ability into MIPs.[5,6] Direct read-out of a binding event without a separation step enables to construct rapid and automated high through-put assays, which is a powerful tool not only for clinical/environmental analysis but also for modern drug discovery.[7] One strategy to introduce signal transduction ability into MIPs is the use of specially designed fluorescent reporter monomers, which change fluorescence emission upon interacting with target molecules.[6] The drawback of this approach is that for each new target molecule, a time-consuming process is often needed to develop a suitable fluorescent monomer. Rather than relying on complicated design and synthesis of different functional monomers, we have previously reported a strategy based on the principle of scintillation proximity assay,[5] where a general-purpose scintillator monomer was incorporated into MIP microspheres. Although the scintillator monomers can be used in different imprinting systems, they require additional aromatic monomers to convert radioisotope decay into short-wavelength emission, which can excite the adjacent scintillator to emit fluorescence. In some cases, co-polymerization of aromatic monomer may not be favorable or even incompatible with obtaining an optimal imprinting effect. Thus, more generally applicable method to introduce signaling ability into MIPs is highly desirable. In this communication, we report a new method for preparation of MIP-based sensing nanofiber materials having signal transduction ability using a simple electrospinning technique.[8] The MIP nanofibers obtained can be readily applied in non-separation assays for detection of a hypertension drug, (*S*)-propranolol.

With this new method, propranolol-imprinted MIP nanoparticles[9] were encapsulated into reporter-doped electrospun polystyrene (PS) nanofibers. The reporter was chosen to offer maximal energy transfer efficiency and not prone to leak from the PS nanofibers. In this way we can easily introduce signal transduction ability into virtually all types of small MIP materials. It allows to synthesize MIPs always under an optimal condition to achieve the best binding sites, and thus makes the method generally applicable to a broad range of target molecules. For comparison, non-imprinted control nanoparticles were also encapsulated into reporter-doped nanofibers and tested.

The principle of proximity scintillation is based on the fact that β-particles emitted from a radioisotope can only travel a short distance in aqueous solution (about 1 μm in the case of ^{3}H).[10] It is only when ^{3}H-labeled analytes are located in proximity of aromatic compounds and scintillator, that the following steps of energy conversion can take place: (1) excitation of aromatic compounds by β-particles, (2) energy transfer from aromatic compounds to the scintillator, and (3) emission of a long-wavelength photon from the scintillator. A schematic illustration of signal transduction in the present proximity scintillation material is shown in Scheme 1.

Polystyrene (PS) was chosen as a supporting polymer matrix since it can provide the function of the aromatic compounds. Using electrospinning, PS nanofibers containing an organic scintillator, 9,10-diphenylanthracene (DPA) were easily obtained. The nanofibers are uniform and randomly oriented, with an average diameter of about 350 nm (see ESI†). Furthermore, DPA-doped nanofibers containing propranolol-MIP nanoparticles (Fig. 1(a)–(c)) and fibers containing control nanoparticles (Fig. 1(d)–(f)) were also prepared using electrospinning. The nanofibers containing nanoparticles have a diameter in the range of 250–500 nm with satisfactorily uniform morphology. The diameter of these nanofibers is slightly increased due to the encapsulation of the nanoparticles, which is in agreement with our previous results when MIP nanoparticles were encapsulated in poly(ethylene terephthalate) fibers.[11] In this work, DPA was incorporated into PS nanofibers without chemical bonding, since its hydrophobic character suggested low possibility of leakage when used in polar or aqueous solvent. Indeed, less than 3% of DPA could

[a] *Pure and Applied Biochemistry, Chemical Center, Lund University, Lund, Sweden. E-mail: Lei.Ye@tbiokem.lth.se; Fax: 46 46 2229560; Tel: 46 46 2224611*
[b] *Swerea IVF, Swedish Institute for Industrial Research and Development, Mölndal, Sweden. E-mail: Ioannis.Chronakis@swerea.se; Fax: 46 31 7066363; Tel: 46 31 7066300*

† Electronic supplementary information (ESI) available: Details of nanoparticle synthesis, electrospinning and scintillation measurement. See DOI: 10.1039/b719586a

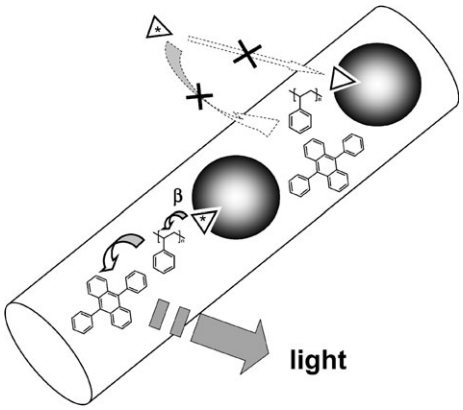

Scheme 1 Schematic representation of proximity scintillation process with composite MIP nanofiber material. Bottom left: when ^{3}H-labeled tracer (triangle with star) binds to the MIP nanoparticle, energy from radioactive decay is transferred into optical signal through the adjacent PS-DPA relay system. Top right: in the presence of an excess of non-labeled analyte (open triangle), ^{3}H-labeled analyte is displaced from the binding site and becomes too distant from the nanofier to achieve effective energy transfer to the PS-DPA system.

be detected in solution after the doped PS nanofibers were incubated in a mixture of 25 mM citrate buffer–acetonitrile (50 : 50, v/v) for 24 h.

The MIP-mediated proximity scintillation was evaluated by incubating the nanofiber materials with 0.246 nM ^{3}H-labeled (*S*)-propranolol in a mixture of 25 mM citrate buffer–acetonitrile (50 : 50, v/v). With the amount of materials increased, the MIP nanofibers produced increasingly higher scintillation signal, and the non-specific signal measured from the control nanofibers remained very weak (Fig. 2). With 5 mg of nanofiber materials, the scintillation signal obtained with the MIP nanofibers (924 cpm) was 3.7-fold of that obtained with the control nanofibers (252 cpm), and 7.2-fold of that obtained with the DPA-doped nanofibers not containing any particles (128 cpm). The scintillation signals from the control nanofibers and the particle-free DPA-doped nanofibers are caused by non-specific adsorption. To confirm that the proximity scintillation signal was generated by MIP-mediated binding, we also measured the amount of free ^{3}H-labeled (*S*)-propranolol remaining in solution using standard liquid scintillation counting. The results were used to calculate the percentage of bound ^{3}H-labeled (*S*)-propranolol (see ESI†), which confirmed that the increase in proximity scintillation signal was caused by specific binding. To further confirm that the present structural assembly of "MIP-nanoparticle/DPA/PS" is essential for efficient signal transduction, we also incubated MIP nanoparticles with ^{3}H-labeled (*S*)-propranolol, and found that no significant scintillation signal could be detected ($<$50 cpm) because of the lack of the PS/DPA. When the particle-free DPA-doped PS nanofibers and the MIP nanoparticles were simultaneously incubated with ^{3}H-labeled (*S*)-propranolol, only a very weak signal (144 cpm) could be observed, indicating the critical importance of confining the binding sites within the DPA-doped PS matrix.

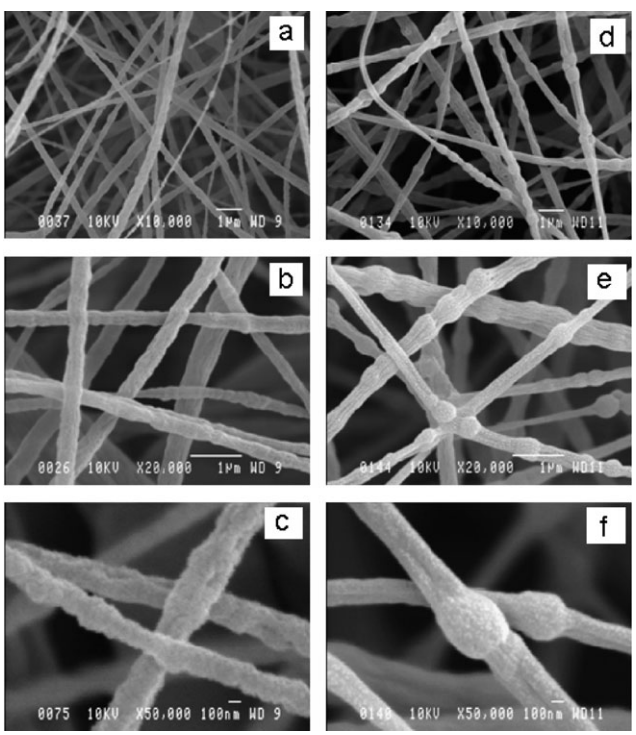

Fig. 1 SEM images of electrospun nanofibers under different magnification: (a–c) DPA-doped PS containing MIP nanoparticles, (d–f) DPA-doped PS containing control nanoparticles.

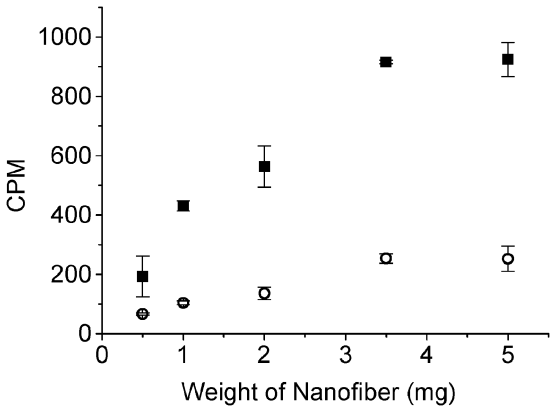

Fig. 2 Proximity scintillation signal (counts per minute, cpm) *vs.* the amount of nanofiber containing MIP nanoparticles (filled squares) and control nanoparticles (open circles). The initial concentration of the ^{3}H-labelled (*S*)-propranolol was 0.246 nM.

Using ^{3}H-labeled (*S*)-propranolol as a tracer, the concentration of (*S*)-propranolol in analytical samples can be determined using competitive binding assays, where the non-labeled (*S*)-propranolol competes with the tracer for the limited number of specific sites in the MIP nanofibers. As shown in Fig. 3, the scintillation signal continued to decrease when an increasing amount of (*S*)-propranolol was added to displace the bound ^{3}H-labeled tracer. From the displacement curve the IC_{50} value of (*S*)-propranolol was estimated to be 16.5 $\pm$ 7.5 μM. The cross-reactivity of several structurally related β-blockers was also calculated from their displacement curves obtained from similar competitive assays (Fig. 3). The obtained cross-reactivity was around 5–10% for (*R*)-propranolol and pindolol, and $<$1% for other tested compounds. Thus, the selectivity of the present proximity scintillation assay is comparable to previous liquid scintillation assay using free

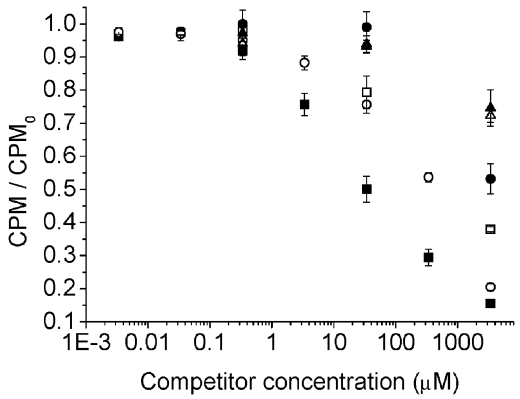

Fig. 3 Displacement curves of ^{3}H-(*S*)-propranolol from nanofibers containing MIP nanoparticles. The mass of the nanofibers used was 2 mg. Competing ligands: (*S*)-propranolol hydrochloride (filled squares), (*R*)-propranolol hydrochloride (open circles), acebutolol hydrochloride (open triangles), pindolol (open squares), metopronolol (+)-tartrate salt (filled circles), atenolol (filled triangles).

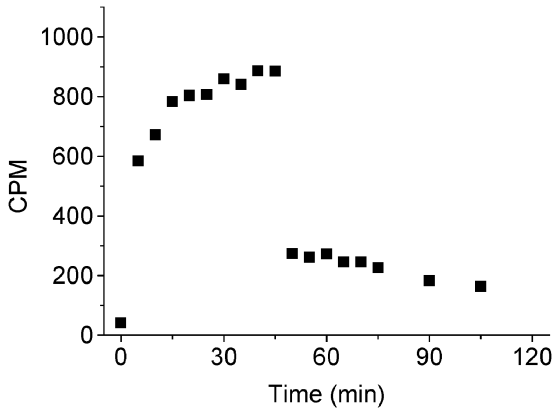

Fig. 4 Real time measurement of binding and dissociation of ^{3}H-labeled (*S*)-propranolol (0.246 nM) with 5 mg of DPA-doped nanofibers containing MIP nanoparticles. The value at 0 min is before the addition of the ^{3}H-labelled (*S*)-propranolol. The dissociation phase started when 34 mM of non-labeled (*S*)-propranolol hydrochloride was added at 45 min.

MIP nanoparticles and tedious separation steps.[9] To demonstrate that the assay can be applied to complex biological samples, we repeated the competitive assays for (*S*)- and (*R*)-propranolol in 10× diluted human urine samples. The IC_{50} value for (*S*)-propranolol hydrochloride (15.5 ± 2.0 μM) and the cross-reactivity towards (*R*)-propranolol hydrochloride (9%) were similar to that obtained in citrate buffer: acetonitrile.

It is interesting to see if encapsulation in PS nanofiber can affect the rate of analyte binding to the MIP nanoparticles, which due to their small physical size have intrinsically fast binding kinetics.[5,12] To follow the time response of the MIP nanofibers, we simply mixed the nanofiber with ^{3}H-labelled (*S*)-propranolol, and made successive counting for the sample at different time intervals. As shown in Fig. 4, the binding reached equilibrium within 30 min, and of the most noteworthy is that the scintillation signal reached 67% of the equilibrium value in less than 5 min. To follow the dissociation of analyte, an excess of non-labelled (*S*)-propranolol hydrochloride was added into the same solution before the sample was further counted. Fig. 4 shows that the signal decreased rapidly by 70% within 5 min, and continued to decrease slowly by another 10% in the following 45 min. A prolonged incubation did not result in further displacement and therefore no complete disappearance of the scintillation signal, which can be explained by the non-specific binding of (*S*)-propranolol to the nanofibers.

In summary, we have developed a simple method for preparation of molecularly imprinted nanofibers having signal transduction ability. This method uses electrospinning to integrate into functional nanofibers all the necessary components needed for proximity scintillation: the MIP nanoparticles, the organic scintillator and the aromatic compound. This method is generally applicable to all types of MIP nanoparticles, possible to provide proximity scintillation nanofibers for analyzing various target compounds as far as they can be successfully imprinted. The electrospun composite nanofibers retain all the favourable properties of MIP nanoparticles, such as high selectivity and very fast binding kinetics. We believe that the new scintillation nanofiber materials reported here can be used to develop high throughput screening assays in several areas including clinical/environmental analysis and in the processes of modern drug development.

This work was supported by the Swedish Foundation for Strategic Research program BIOMICS (Lund University) and the Swedish Research Council program IRECO Holding (Swerea IVF).

Notes and references

1 K. Haupt and K. Mosbach, *Chem. Rev.*, 2000, **100**, 2495; G. Wulff, *Chem. Rev.*, 2002, **102**, 1; L. Ye and K. Haupt, *Anal. Bioanal. Chem.*, 2004, **378**, 1887.
2 J. Svenson and I. A. Nicholls, *Anal. Chim. Acta*, 2001, **435**, 19.
3 I. Tokareva, I. Tokarev, S. Minko, E. Hutter and J. H. Fendler, *Chem. Commun.*, 2006, 3343.
4 J. Matsui, T. Sodeyama, K. Tamaki and N. Sugimoto, *Chem. Commun.*, 2006, 3217.
5 L. Ye and K. Mosbach, *J. Am. Chem. Soc.*, 2001, **123**, 2901; L. Ye, I. Surugiu and K. Haupt, *Anal. Chem.*, 2002, **74**, 959; L. Ye, *Mater. Res. Soc. Symp. Proc.*, 2003, **787**, 97.
6 T. Takeuchi, T. Mukawa and H. Shinmori, *Chem. Rec.*, 2005, **5**, 263; C. J. Stephenson and K. D. Shimizu, *Polym. Int.*, 2007, **56**, 482.
7 G. S. Sittampalam, S. D. Kahl and W. P. Janzen, *Curr. Opin. Chem. Biol.*, 1997, **1**, 384; L. Silverman, R. Campbell and J. R. Broach, *Curr. Opin. Chem. Biol.*, 1998, **2**, 397; A. Smith, *Nature*, 2002, **418**, 453.
8 D. H. Reneker and I. Chun, *Nanotechnology*, 1996, **7**, 216; Y. Dzenis, *Science*, 2004, **304**, 1917; D. Li and Y. Xia, *Adv. Mater.*, 2004, **16**, 1151.
9 K. Yoshimatsu, K. Reimhult, A. Krozer, K. Mosbach, K. Sode and L. Ye, *Anal. Chim. Acta*, 2007, **584**, 112.
10 H. E. Hart and E. B. Greenwald, *Mol. Immunol.*, 1979, **16**, 265; S. Udenfriend, L. Gerber and N. Nelson, *Anal. Biochem.*, 1987, **161**, 494; N. Bosworth and P. Towers, *Nature*, 1989, **341**, 167.
11 I. S. Chronakis, A. Jakob, B. Hagström and L. Ye, *Langmuir*, 2006, **22**, 8960.
12 L. Ye, P. A. G. Cormack and K. Mosbach, *Anal. Commun.*, 1999, **36**, 35.

